Correction of cirrus effects in Sentinel-2 type of imagery

RUDOLF RICHTER; XINGJUAN WANG, MARTIN BACHMANN

German Aerospace Center (DLR)
German Remote Sensing Data Center (DFD)
D – 82234 Wessling, Germany

DANIEL SCHLÄPFER
ReSe Applications
Langeggweg 3
CH – 9500 Wil, Switzerland

shortened version of title (running head): **Cirrus correction in Sentinel-2 type of imagery**

Email of corresponding author: Rudolf.Richter@dlr.de

Abstract

Optical satellite images are often contaminated with cirrus clouds. Thin cirrus can be detected with a channel at 1.38 μm, and an established cirrus removal method exists for visible/near-infrared (VNIR) channels in atmospheric window regions which was demonstrated with MODIS (Moderate Resolution Imaging Spectrometer) data. This contribution addresses open issues of cirrus correction for Sentinel-2 type of instruments, i.e., future spaceborne sensors such as Sentinel-2 or similar instruments. These issues are (i) an extension of the existing technique to account for cirrus during the water vapour retrieval (channel at 0.94 μm) and surface reflectance calculation to avoid reflectance artefacts at 0.94 μm, (ii) a discussion of options concerning cirrus removal in the short-wave infrared (SWIR, channels at 1.6 and 2.2 μm) region, and (iii) an analysis of channel parallax (view angle) requirements to achieve a high quality cirrus removal.

1   Introduction

Thin cirrus clouds are difficult to detect in imagery from typical broad-band multispectral satellite sensors, especially over land, because land scenes are spatially inhomogeneous and this type of cloud is partially transparent. Cirrus clouds typically occur in the upper troposphere and lower stratosphere, i.e., in altitudes of 7 – 20 km. On the other hand, water vapour dominates in the lower troposphere, and usually 90% or more of the atmospheric water vapour column is located in the 0 – 6 km altitude layer. Therefore, if a narrow spectral band is selected in a spectral region of very strong water vapour, e.g., around 1.38 µm or 1.88 µm, the ground reflected signal will be totally absorbed, but the scattered cirrus signal will be received at a satellite sensor or an instrument operating in a high-altitude aircraft (Gao *et al.*, 1998, 2002). Such a channel at 1.38 µm is able to detect cirrus, and if a correlation of the cirrus signal at this wavelength and other wavelengths in the VNIR regions can be found, then the cirrus contribution can be removed from the radiance signal to obtain a cirrus-corrected scene. This idea is exploited in the state-of-the-art algorithm applied to AVIRIS (Airborne Visible/Infrared Imaging Spectrometer, Vane *et al.* 1993) and MODIS data (Gao *et al.* 1998, 2002). It works in the atmospheric window regions of the VNIR spectrum.

Open issues are the treatment of a VNIR absorption channel (i.e., 0.94 µm) and SWIR window channels (around 1.6 µm and 2.2 µm). To our knowledge this contribution is also the first to study the influence of different channel parallax angles (view directions) and it proves that a high quality cirrus removal requires parallax angles smaller than 1 pixel at the typical range of cirrus heights (7 – 20 km).

The proposed improvements aim at a new generation of multispectral instruments such as Sentinel-2 (ESA 2010), a member of the Sentinel family in the frame of Global Monitoring for Environment and Security (GMES). Sentinel-2 has VNIR bands, a water vapour channel in the 0.94 µm region, a cirrus channel at 1.38 µm, and SWIR channels in the 1.6 µm and 2.2 µm regions. The removal of cirrus contamination in all bands is important for improving the accuracy of surface reflectance retrievals and subsequent higher level products. Table 1

contains the spectral bands of Sentinel-2. In this study we use 12 bands, the panchromatic band B8 is not considered because it is not required for the analysis of the spectral information in the data as a narrow band B8a is available in the NIR region.

Place Table 1 here.

The processing example (sections 4 and 6) takes the spectral / spatial characteristics of Sentinel-2 as a template for instruments with similar properties as Sentinel-2 to investigate the relevant cirrus effects. It is not intended and not necessary to reproduce exactly all Sentinel-2 features to discuss the critical points for the cirrus removal. Instead, the objective is to achieve a general assessment of requirements concerning cirrus removal for instruments similar to Sentinel-2.

2   Standard cirrus removal method

We first need a brief discussion of the standard cirrus removal method (Gao *et al.* 1998, 2002) to understand the proposed enhancements. In Gao *et al.* (2002, Fig. 1) a "virtual" surface is defined consisting of the earth's surface and atmosphere beneath cirrus clouds. It includes the effects of surface reflection and atmospheric scattering and absorption processes. Above cirrus there is the remaining part of the atmosphere with a residual water vapour column. For thin cirrus the following relationship was derived for atmospheric window regions:

$$\rho^*(\lambda) = \rho_c(\lambda) + T_c(\lambda)\rho_v(\lambda) \tag{1}$$

where ρ^* denotes a top-of-atmosphere (TOA) reflectance, λ is the channel centre wavelength, $\rho_c(\lambda)$ is the cirrus reflectance, T_c is the two-way transmittance through the cirrus and ρ_v is the reflectance of the "virtual surface" below the cirrus. With the assumption that the cirrus reflectance $\rho_c(\lambda)$ in the VNIR (from 0.4 to 1 µm) is linearly related to the cirrus reflectance at 1.38 µm, i.e., $\rho_c(\lambda) = \rho^*_{1.38}\, g$ we obtain:

$$T_c\,\rho_v(\lambda) = \rho^*(\lambda) - \rho^*_{1.38}\, g \qquad (0.4 < \lambda < 1.0\,\mu m) \tag{2}$$

The μm unit in reflectance subscripts is omitted for brevity. The empirical parameter g is derived from a scene scatterplot of the 1.38 μm cirrus channel versus a red (around 0.66 μm) channel (Gao *et al.* 2002, Fig.'s 2, 5, 8) and it is related to the transmittance for water vapour, T_{H2O}, at 1.38 μm above and within cirrus clouds:

$$T_{H2O}(1.38) = 1/g \qquad (3)$$

T_c is typically greater than 0.9 and is approximated by a value of 1.

$$\rho_v(\lambda) = \rho^*(\lambda) - \rho^*_{1.38}\, g = \rho^*(\lambda) - \frac{\rho^*_{1.38}}{T_{H2O}(1.38)} \qquad (4)$$

Equation (4) with $g=g(VNIR)$ is the basis for the standard cirrus removal. It is restricted to the VNIR region, because the cirrus single scattering albedo (SSA) is close to 1 in this part of the spectrum (Baum *et al.* 2005, see Fig.1) which means that scattering dominates. It does not hold in the SWIR spectrum (1.6 μm, 2.2 μm) where cirrus absorption is higher, i.e., SSA < 1. So far, eq. (4) has only been applied to channels in VNIR window regions, excluding the 0.94 μm water vapour region. The next section describes an enhanced cirrus removal including a treatment of the 0.94 μm absorption channel.

Place Figure 1 here

3   Cirrus removal in the 0.94 μm region

The enhanced method accounts for the water vapour absorption above cirrus clouds for the 0.94 μm water vapour channel during the water vapour retrieval and surface reflectance calculation. Although the two-way transmittance (sun-cirrus-sensor) $T_{H2O}(0.94)$ is relatively high (typical values range around 0.95, depending on cirrus height), this effect cannot be neglected as shown in section 5, because it influences the overall water vapour column on which the surface reflectance calculation critically depends. Therefore, if this effect is taken into account, the surface reflectance in the 0.94 μm channel is much closer to expected values and severe artefacts in the reflectance spectrum can be avoided (see section 5).

For instruments with similar channels as Sentinel-2 the water vapour is retrieved with a band in a window region (around 0.87 µm) and one in the 0.94 µm absorption region. In the window channel the cirrus signal is accounted for as described in eq. (4). In an absorption region ($\lambda = \lambda_a = 0.94$ µm) eq. (1) has to be modified to include the two-way transmittance sun-cirrus-satellite $T_{H2O}(\lambda_a)$ of the water vapour column above cirrus. The corresponding equation is

$$\rho^*(\lambda_a) = \left(\rho_c(\lambda_a) + T_c(\lambda_a)\,\rho_v(\lambda_a)\right)\,T_{H2O}(\lambda_a) \tag{5}$$

With the approximation $T_c(\lambda_a) = 1$ and $\rho_c(\lambda_a) = \rho^*_{1.38}\,/\,T_{H2O}(1.38)$ we obtain

$$\rho_v(\lambda_a) = \frac{\rho^*(\lambda_a)}{T_{H2O}(\lambda_a)} - \frac{\rho^*_{1.38}}{T_{H2O}(1.38)} \tag{6}$$

Although T_{H2O} (for $\lambda_a = 0.94$ µm) is initially not known, one can calculate the ratio $R = T_{H2O}(0.94)\,/\,T_{H2O}(1.38)$ with a radiative transfer code using climatologic profiles (mid-latitude summer, winter, US standard) of height, pressure, temperature, and water vapour for a typical cirrus height range (7 – 20 km), nadir view, and different solar geometries (solar zenith angles from 0 – 70°). An example is shown in Fig. 2(a) where the two-way transmittance (sun-cirrus-sensor) is plotted for the mid-latitude summer (MS), mid-latitude winter (MW), and US standard atmospheres (MODTRAN code, Berk *et al.* 1998) for a nadir-looking sensor and a solar zenith angle of 30°.

Place Fig. 2 here

The dashed line indicates a transmittance value $T_{H2O}(1.38\mu m) = 0.6$. For the MS atmosphere this value represents a cirrus height of 9 km, while it corresponds to a height of 7.5 km and 8 km for the MW and US atmospheres, respectively. However, Fig. 2(b) shows that the transmittances $T_{H2O}(0.94$ µm) as a function of $T_{H2O}(1.38$ µm) are almost the same for these three atmospheres, so the ratio R is almost independent of the selected climatologic atmosphere and look-up tables (LUTs) of the two-way transmittances and ratios can be compiled with a fixed atmosphere (e.g. US standard). With these LUTs and a knowledge of

$T_{H2O}(1.38)$ (from the scene scatterplot $\rho^*_{1.38}$ versus $\rho^*_{0.66}$, see Fig. 2 of Gao *et al.* 2002) the ratio R can be calculated. Then eq. (6) can be written as

$$\rho_v(\lambda_a) = \frac{\rho^*(\lambda_a)}{R\, T_{H2O}(1.38)} - \frac{\rho^*_{1.38}}{T_{H2O}(1.38)} \tag{7}$$

which is the counterpart of eq. (4) for the absorption channel.

4   Cirrus removal for 1.6 µm and 2.2 µm channels

In the VNIR region thin cirrus always increases the apparent reflectance over dark and bright surfaces because the cirrus single scattering albedo is close to 1 (see Fig. 1). However, the equations (4, 7) cannot be applied to channels in the 1.6 µm and 2.2 µm region where cirrus has scattering and absorption properties. This means in the SWIR regions cirrus increases the apparent reflectance over dark surfaces (scattering properties dominate), while cirrus can decrease the apparent reflectance over bright surfaces if the absorption effect is stronger than the scattering. This fact poses a problem for the consistent calculation of surface reflectance spectra, and there exist three possibilities to handle this situation: (a) no cirrus removal is conducted yielding a degraded image quality reflectance, (b) cirrus removal is only conducted for the VNIR bands yielding inconsistent reflectance spectra in the SWIR, and (c) cirrus removal is conducted over the whole spectrum using an empirical correction factor for the SWIR bands.

We propose the optional use of the empirical factor 0.5 g in equation (4) for SWIR channels to avoid small or negative surface reflectance values for dark surfaces. It is a compromise until better solutions can be found.

5   Results

For the simulation of Sentinel-2 channels we use data acquired by AVIRIS (Vane *et al.* 1993) which is spectrally resampled with the Sentinel-2 response curves. The sample AVIRIS scene was recorded on July 7, 1996 over Bowie, Maryland, near a latitude of 38.97° N and a longitude of 76.74° W. The flight altitude is 20 km and the solar zenith angle is 31.3°. Except

for the effect of the absorption in the ozone layer (20 – 40 km altitude), the 20 km high altitude AVIRIS scenes are a good approximation of data from spaceborne platforms. For the purpose of this investigation, we keep the 20 m spatial resolution of AVIRIS for all simulated Sentinel-2 channels except for the bands at 0.443 μm, 0.945 μm, and 1.375 μm which are resampled to 60 m using a 3×3 pixel low pass filter. A use of the corresponding Sentinel-2 channel point spread function (PSF) is not necessary to demonstrate the critical cirrus effects as it would lead to very similar results in spatially homogeneous areas. In inhomogeneous areas somewhat larger differences will be encountered (as the PSF includes contributions from distances farther away) which would only confirm the findings of this study on critical issues. So the resampled scene is similar to a Sentinel-2 scene (same spectral channels), but not identical (the 60 m bands do not have the Sentinel-2 PSF's).

Place Figure 3 here

Figure 3a shows a small sub-scene of size 614 columns and 438 lines representing an area of 12.240 km by 8.760 km. Fig. 3b represents the corresponding apparent cirrus reflectance $\rho^{*}_{1.38}$ at 1.38μm. The two water vapour maps are calculated with the standard method (Fig. 3c, ignoring the cirrus) and with the enhanced method (Fig. 3d, cirrus contribution subtracted from the TOA radiance), respectively. The water vapour retrieval is calculated with the atmospheric precorrected differential absorption technique (Schläpfer et al. 1998).

The standard water vapour product (Fig. 3c) shows a high (negative) correlation between water vapour column and cirrus intensity (coefficient of determination $R^2 = 0.79$), because thin cirrus clouds partly mask the water vapour beneath. With the enhanced method the correlation drops to $R^2 = 0.12$, i.e. water vapour and cirrus maps achieve a significantly better decorrelation. Fig. 3e presents a true colour rendition of the surface reflectance of the scene after cirrus removal and atmospheric correction (performed with the ATCOR model, Richter 1998).

Fig. 3a marks six target locations (T1 to T6) of various thin cirrus intensity from which surface reflectance spectra are extracted (Fig. 4). The purpose is to illustrate the spectral behaviour for different processing options (P0 to P3) and cirrus optical thicknesses:

- (P0) ignoring cirrus during water vapour and surface reflectance retrievals,

- (P1) standard cirrus correction: ignoring cirrus during water vapour calculation, but applying cirrus removal with eq. (4) for the VNIR bands (diamond symbol and green line in the $0.87 - 1.6$ µm region),
- (P2) enhanced cirrus method: cirrus accounted for during water vapour and surface reflectance calculation with factor g (eq. 4) applied to all bands (diamond symbol and red line in the 1.6, 2.2 µm region),
- (P3) same as (P2), but with g(SWIR)= 0.5 g (diamond symbol, black line at 1.6, 2.2 µm).

Place Figure 4 here

The spectra (Fig. 4a to 4f) show major artefacts for the processing options (P0), (P1). Spectra calculated with (P1) show dips at 0.94 µm caused by neglecting the water vapour influence T_{H20}(0.94 µm) = 0.95. The corresponding surface reflectance error depends on surface type, the neighbourhood (because of the adjacency effect) and cirrus intensity and ranges between 0.10 to 0.18 reflectance units for the selected target spectra in Fig. 4, compare (P3) spectra. Option (P2) leads to unreasonably low reflectance values for dark surfaces in the 1.6 µm and 2.2 µm bands, (P3) avoids this behaviour at the price of an empirical adjustment factor (see discussion section). The cirrus band (1.38 µm) is not included in the spectra as no surface information can be retrieved in this band.

Parallax issue:

A potential problem for the cirrus removal technique exists if the channels have different parallax angles (view directions). Parallax differences of AVIRIS data are negligible, so the resampled data used here for the simulation of a Sentinel-2 similar system are also negligible. However, different channel-dependent parallaxes exist for the actual Sentinel-2 instrument (GMES 2009). To simplify the following brief sensitivity investigation and to make a general statement, we assume the same parallax angles for all bands except for the cirrus band (60 m resolution), and we vary the cirrus band parallax in such a way that it corresponds to displacements of 1, 3, and 5 scene pixels based on the 20 m resolution bands. Therefore, we purposely do not apply it to Sentinel-2 in the following Figure 5, but to a simulated similar instrument, to stress the critical issue and enable a general assessment.

Figure 5 (a zoomed subset of Fig. 3) shows the influence of a parallax error of 1, 3, and 5 pixels (with 20 m) between the cirrus channel (1.38 μm) and the remaining channels. Even for a 1 pixel misregistration the cirrus removed product is slightly degraded, and its quality is severely degraded for misregistrations of 3 pixels or more.

Place Figure 5 here

Figure 6 shows the parallax effect for the actual Sentinel-2 instrument for cirrus heights of 10 km and 20 km using the 1.38 μm cirrus band as reference. Depending on cirrus height, a large number of channels does not fulfill the criterion of a spatial misregistration smaller than 1 or 2 pixels.

Place Figure 6 here

6   Discussion

The previous section presented results for an enhanced method of cirrus removal. Two improvements were made: the above-cirrus water vapour is considered during the water vapour retrieval (0.94 μm channel) and during the surface reflectance retrieval in this channel leading to a more accurate assessment of the water vapour map and avoiding spikes at 0.94 μm in the surface reflectance spectra.

As part of the enhanced method, LUTs with radiative transfer calculations of the water vapour transmittances $T_{H2O}(0.94\mu m)$ and $T_{H2O}(1.38\mu m)$ above cirrus are compiled as a function of cirrus height and solar/observation geometry. With a knowledge of $T_{H2O}(1.38\mu m)$ for the current geometry (scene scatterplot of $\rho_{1.38}^*$ versus $\rho_{0.66}^*$, Fig. 2 of Gao *et al.* 2002), the apparent cirrus height can be estimated for the selected standard atmosphere, subsequently the ratio $R = T_{H2O}(0.94\mu m) / T_{H2O}(1.38\mu m)$, and then $T_{H2O}(0.94\mu m)$. This ratio is independent of the selected atmosphere, but different apparent cirrus heights are obtained for different atmospheres. For cirrus heights above 12 km the 2-way transmittance $T_{H2O}(0.94\mu m)$ is greater than 0.99 and the term $R\ T_{H2O}(1.38\mu m)$ of eq. (7) tends to 1 yielding eq. (4) as a special case of eq. (7). So for high cirrus clouds eq. (4) is accurate enough, but for lower clouds (below approximately 12 km) eq. (7) has to be used. As the cirrus height in a scene is generally not

known, the use of eq. (7) is recommended to be on the safe side. The limitation of the method is that the cirrus height is assumed to be the same per scene.

A problem exists for the cirrus removal in the SWIR bands (1.6, 2.2 μm). Contrary to the VNIR region where the cirrus single scattering albedo SSA is close to 1 (i.e., scattering dominates) the SWIR part of the spectrum has to consider cirrus absorption properties as well (SSA < 1). For instruments with the Sentinel-2 set of channels there is currently no method to cope with this problem. If a cirrus removal is conducted for VNIR and not for SWIR bands (current approach), the SWIR part of the spectrum is inconsistent with the VNIR part. If the SWIR surface reflectance is calculated on the same basis as for the VNIR (i.e. SSA = 1) the values are too low and can even become negative for dark surfaces (vegetation). Therefore, we propose a compromise with an empirical cirrus adjustment factor until a better solution is available.

Concerning different channel parallaxes: parallax differences can be corrected if the distance (sensor to Earth surface) is known. The effect cannot be taken into account for unknown cirrus altitudes. It is demonstrated that a high-quality cirrus removal requires that parallax angle differences between all channels be less than 1 pixel for the typical height range of cirrus. If the parallax effect at the cirrus cloud height is 3 pixels or more the cirrus removed product is severely degraded and the profit of such a product is questionable. This poses a problem for the actual Sentinel-2 processing.

In principle, the parallax problems could be handled by iterating the complete processing chain: at the start when calculating the level-1 TOA radiance product, the parallax differences are taken into account as usual based on the current geometry. After atmospheric correction (including cirrus removal) the approximate cirrus height can be estimated (±1 km, assumption: same cirrus height for all pixels). Then the level-1 product is updated using the cirrus mask and height information to calculate different parallax compensations for the non-cirrus and cirrus-affected pixels. The last step iterates the atmospheric correction. More work is needed to implement such a correction in an operational processing chain.

7   Conclusions

An enhanced cirrus removal method for thin cirrus is presented for the next generation multispectral instruments with channels in the VNIR region including a water vapour band (around 0.94 µm), a cirrus band (around 1.38 µm), and SWIR bands at 1.6 µm and 2.2 µm. The method accounts for water vapour above cirrus in the 0.94 µm channel during the water vapour and surface reflectance retrievals, and therefore avoids cirrus induced surface reflectance artefacts in the 0.94 µm region. In addition to the radiative transfer LUTs required for water vapour and surface reflectance retrieval, the method requires further LUTs containing the ratio $R = T_{H2O}(0.94\mu m) / T_{H2O}(1.38\mu m)$ of above-cirrus transmittances for different solar and viewing conditions. This ratio is independent of the selected atmosphere and needed to calculate the transmittance $T_{H2O}(0.94\mu m)$.

As an alternative to current approaches the optional use of an empirical scale factor for the cirrus removal in the SWIR region is presented to avoid an overcorrection of surface reflectance for dark surfaces.

The method has been applied to simulated scenes of the Sentinel-2 type, but can generally be used for instruments with similar spectral bands. It is demonstrated that a high quality cirrus removal can only be achieved when the channel parallax differences are smaller than 1 pixel at the typical range of cirrus heights. This poses a problem for the processing of actual Sentinel-2 imagery because about half of the channels have relatively large parallax angle differences with respect to the cirrus band

References

BAUM, B. A., HEYMSFIELD, A. J., YANG, P., and BEDKA, S. T., 2005, Bulk scattering properties for the remote sensing of ice clouds. Part I: Microphysical data and models. *Journal of Applied Meteorology*, **44**, pp. 1885-1895.

BERK, A., BERNSTEIN, L. S., ANDERSON, G: P., ACHARYA, P. K., ROBERTSON, D. C., CHETWYND, J. H., and ADLER-GOLDEN, S. M., 1998, MODTRAN cloud and multiple scattering upgrades with application to AVIRIS. *Remote Sensing of Environment,* **65**, pp. 367-375.

ESA team, 2010, GMES Sentinel-2 mission requirements document. http://www.esamultimedia.esa.int/docs/GMES/Sentinel-2_MRD.pdf .

GAO, B.-C., KAUFMAN, Y. J., HAN, W., and WISCOMBE, W. J., 1998, Correction of thin cirrus path radiances in the 0.4 – 1.0 µm spectral region using the sensitive 1.375 cirrus detecting channel. *Journal of Geophysical Research*, **103**, No. D24, pp. 32,169-32,176.

GAO, B.-C., YANG, P., HAN, W., LI, R.-R., and WISCOMBE, W. J., 2002, An algorithm using visible and 1.38 µm channels to retrieve cirrus cloud reflectances from aircraft and satellite data, *IEEE Transactions on Gesscience and Remote Sensing*, **40**, pp. 1659-1668.

GMES Sentinel-2 team, 2009, GMES Sentinel-2 System Requirements Document S2-SRD-B2CDE1_Revised_11112009_signed.pdf .

RICHTER, R., 1998, Correction of satellite imagery over mountainous terrain, *Applied Optics*, **37**, pp. 4004-4015.

SCHLÄPFER, D., BOREL, C. C., KELLER, J., and ITTEN, K. I., 1998, Atmospheric precorrected differential absorption technique to retrieve columnar water vapor. *Remote Sensing of Environment*, **65**, pp. 353-366.

VANE, G., GREEN, R. O., CHRIEN, T. G., ENMARK, H. T., HANSON, E. G., and PORTER, W. M., 1993, The Airborne Visible/Infrared Imaging Spectrometer (AVIRIS). *Remote Sensing of Environment,* **44**, pp. 127-143.

band	centre wavelength (μm)	bandwidth (nm)	spatial resolution (m)
1	0.443	20	60
2	0.490	65	10
3	0.560	35	10
4	0.665	30	10
5	0.705	15	20
6	0.740	15	20
7	0.783	20	20
8	0.842	115	10
8a	0.865	20	20
9	0.945	20	60
10	1.375	30	60
11	1.610	90	20
12	2.190	180	20

Table 1.   Spectral bands and spatial resolution of Sentinel-2 (ESA 2010).
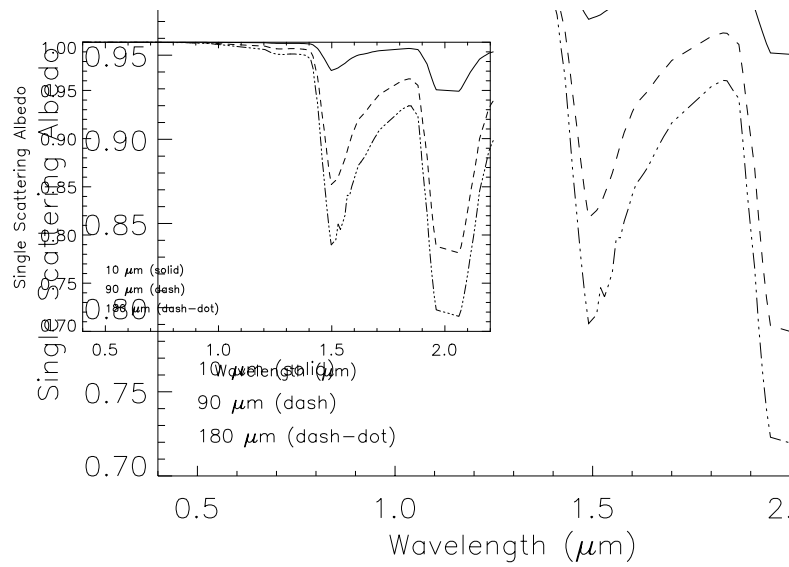
Figure 1 Single scattering albedo of cirrus for three effective particle diameters (Baum *et al.* 2005).
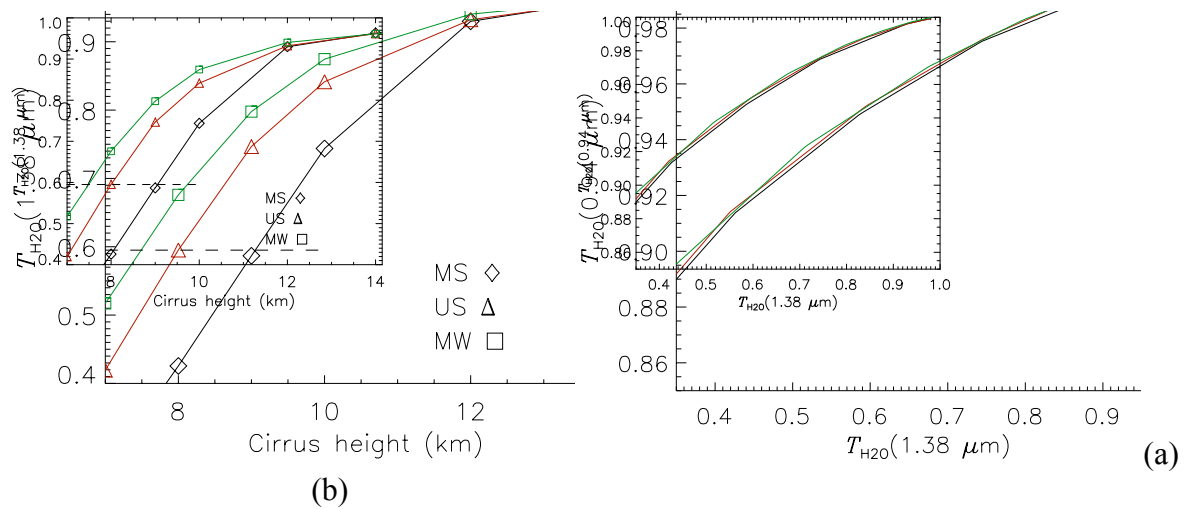
Figure 2 (a) Two-way transmittance $T_{H2O}(1.38\mu m)$ sun-cirrus-sensor for the mid-latitude summer (MS), mid-latitude winter (MW), and US standard atmospheres, nadir view, solar zenith angle 30°. The dashed line indicates a scene-derived transmittance.
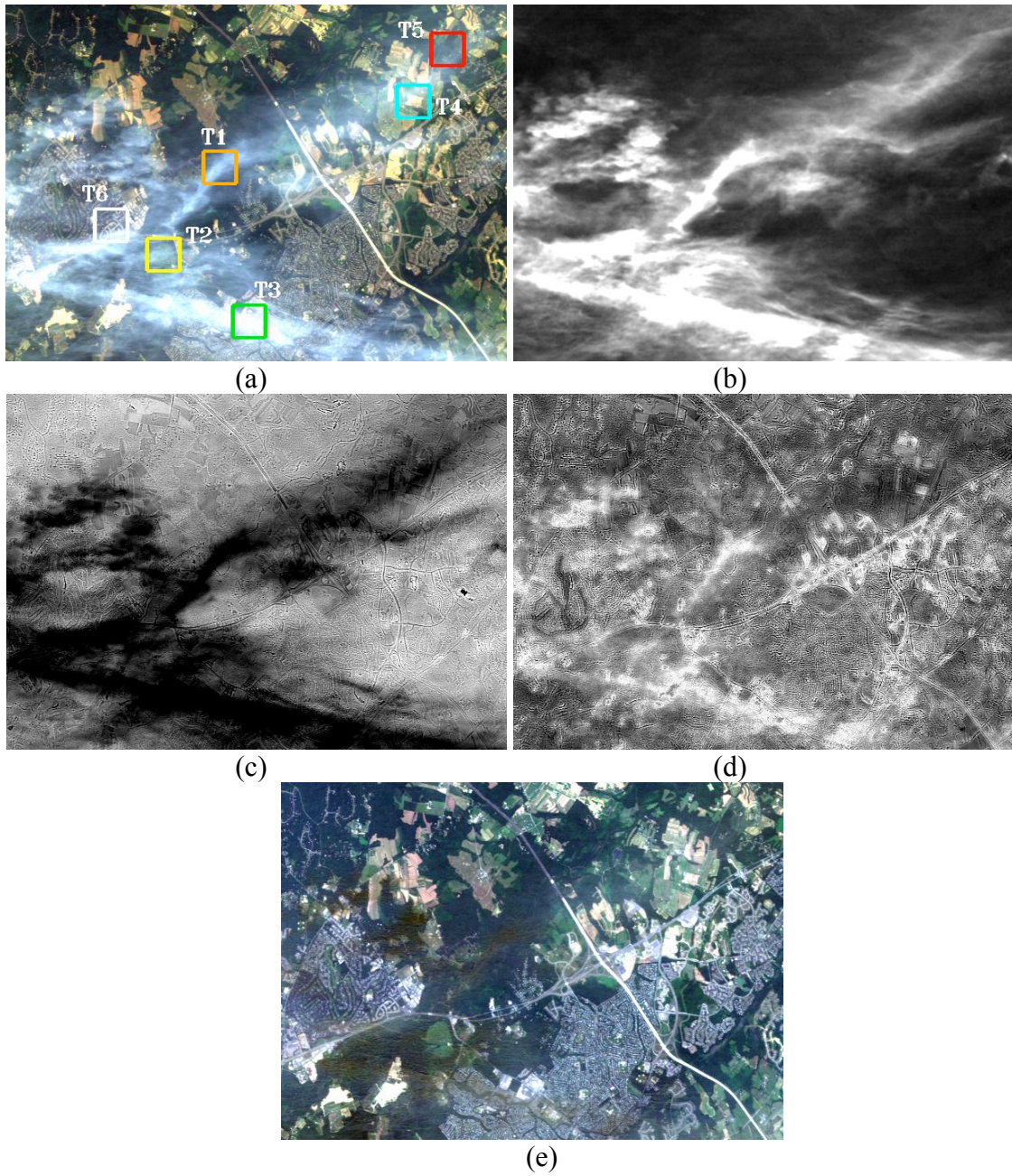(b) Transmittance $T_{H2O}(0.94\mu m)$ as a function of $T_{H2O}(1.38\mu m)$ for the MS, MW, and US atmospheres coded as black, green, and red, respectively.

Figure 3 (a) Original scene Red/Green/Blue = 0.66/0.56/0.49 μm, (b) values of cirrus $\rho^*(1.38\mu m)$, black; value close to zero, white; value 0.03 or higher,
(c) water vapour ignoring cirrus during retrieval, (d) water vapour accounting for cirrus,
(e) cirrus-corrected surface reflectance image. T1 to T6 are target locations for spectra in Fig. 4.
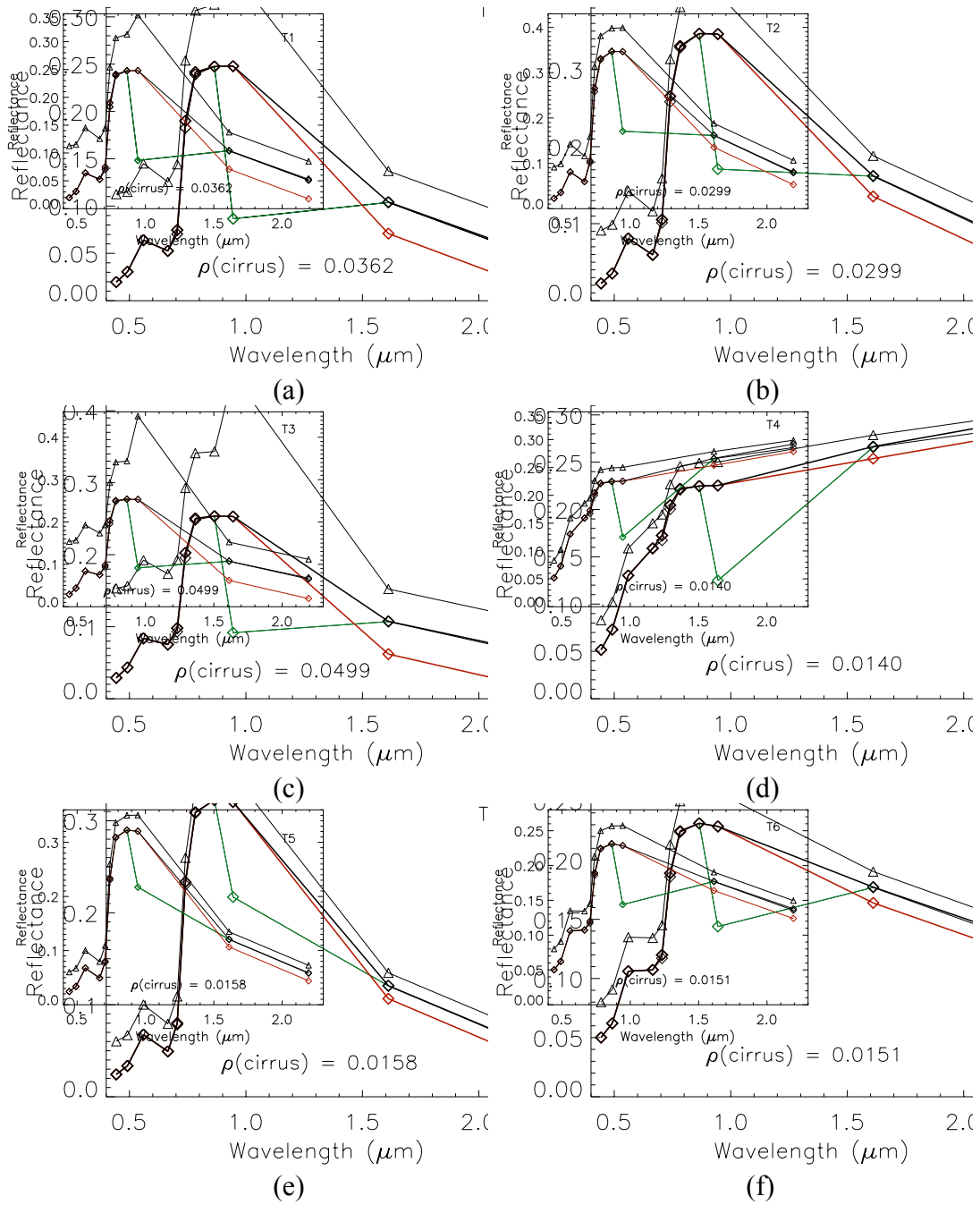
Fig. 4 Retrieved surface reflectance spectra from different locations of Fig. 1. Triangle: method P0, diamond and green (P1), diamond and red (P2), diamond and black for all bands (P3), see text for details.

16

(a)   (b)
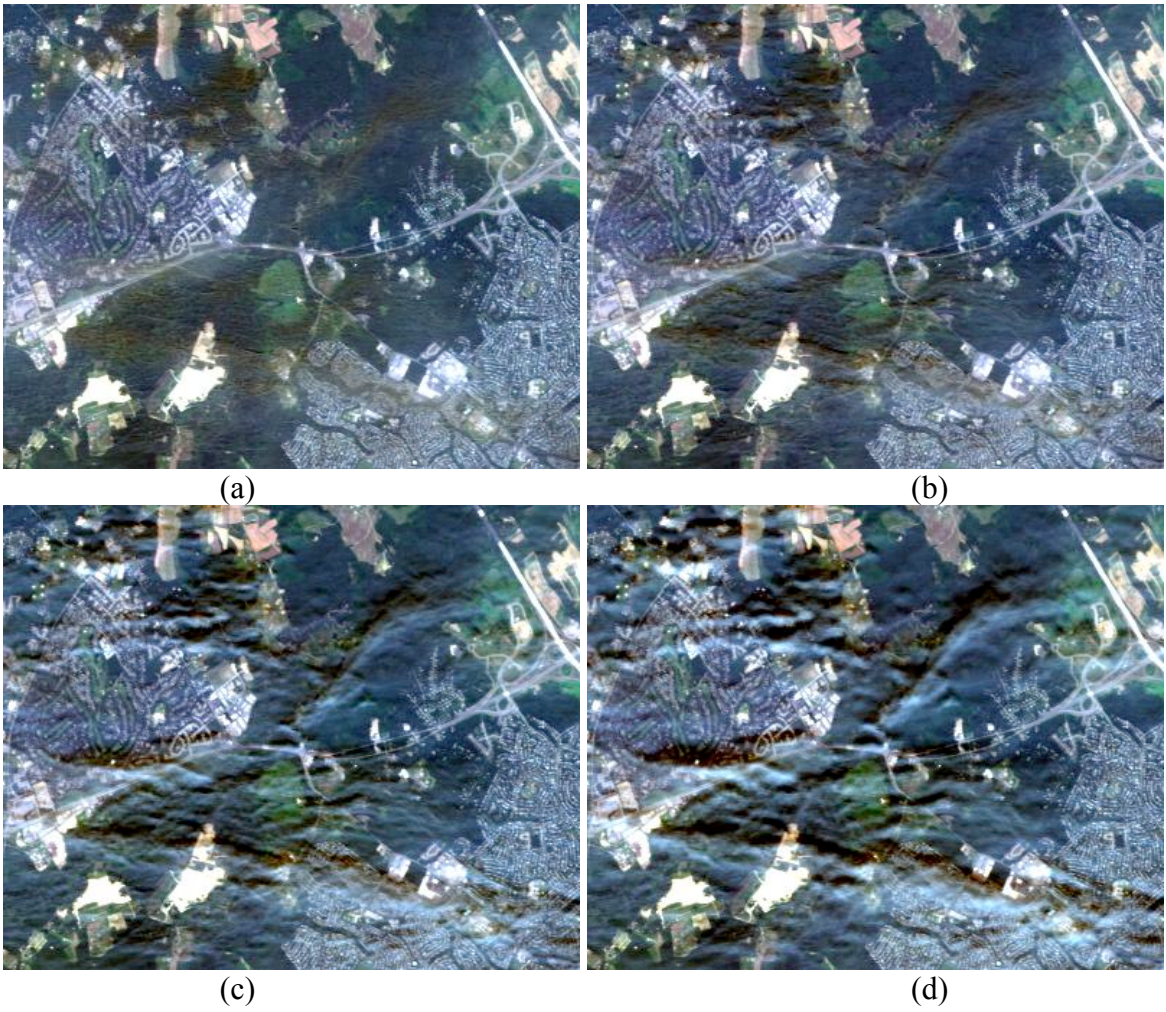
(c)   (d)

Figure 5   Subset of Fig. 3 scene demonstrating the influence of parallax differences (a) no parallax, (b), (c), (d) parallax 1, 3, 5 pixels, respectively.
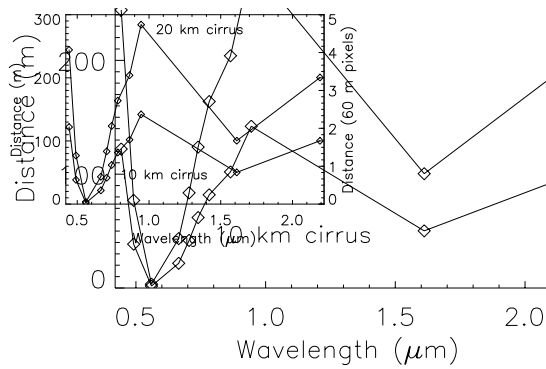

Figure 6   Parallax effect for the actual Sentinel-2 instrument for two cirrus cloud heights.